Materials Advances

ROYAL SOCIETY OF CHEMISTRY

PAPER

View Article Online
View Journal | View Issue

Cite this: *Mater. Adv.*, 2026, 7, 5106

Suppressing the non-radiative energy loss in non-fullerene-based organic solar cells *via* solid additives of racemic and isotactic nitroxide radical polymonothiocarbonates

Yuyan Tao,†[a] Xuanyu Zhou,†[a] Xiao Zheng,[a] Huiyuan Peng,[a] Min Gyu Kang,[c] Pengzhi Guo,[a] Xunchang Wang,[b] Renqiang Yang,[b] Ergang Wang,[d] Hanyoung Woo[c] and Yangjun Xia*[a]

The larger non-radiative energy loss ($\Delta V_{oc}^{non\text{-}rad}$) of the non-fullerene-based organic solar cells (NFAs-OSCs) has been demonstrated to be the main barrier to further boosting the efficiency of NFAs-OSCs. In response, extensive studies have been implemented, focusing on the optimization of the photoactive layer morphology, molecular engineering of donors and acceptors, and the development of multi-component NFAs-OSCs *etc.*, thereby achieving a series of devices with markedly enhanced performance. As an emerging strategy, the utilization of nitroxide radical-conjugated polymer additives is also worthy of attention due to their ability to simultaneously enhance the performance and stability of NFAs-OSCs. In this study, the racemic and isotactic nitroxide radical polymonothiocarbonates (PTC-NOs, with the specific names of *Rac*-PTC-NO, (*R*)-PTC-NO and (*S*)-PTC-NO) are employed as solid additives to mitigate the $\Delta V_{oc}^{non\text{-}rad}$ of the NFAs-OSCs. Upon the addition of 0.5 wt% of *Rac*-PTC-NO, (*R*)-PTC-NO and (*S*)-PTC-NO, the PCEs of the PM6:Y6-based NFAs-OSCs are respectively improved from 15.73% to 16.59%, 17.30% and 17.40%. Besides, the reasons behind the improvement in the performance of the NFAs-OSCs from the representative photovoltaic material pair of PM6:Y6, such as the increase of the exciton dissociation probability, suppression of charge carrier recombination and mitigation of the non-radiative energy loss of the devices upon the addition of the PTC-NOs additives, are supported by and discussed through a set of comparative investigations. This work not only broadens the scope but also provides new insights for designing and developing efficient nitroxide radical-based polymeric additives to mitigate the non-radiative energy loss, thus further boosting the performance of NFAs-OSCs.

Received 13th January 2026,
Accepted 28th March 2026

DOI: 10.1039/d6ma00058d

rsc.li/materials-advances

1. Introduction

Since the discovery of the ultra-fast photo-induced charge transfer between conjugated polymers and fullerene, and the pioneering development of bi-continuous network bulk heterojunction organic solar cells in the early 1990s,[1,2] organic solar cells (OSCs) with a thin film of nanostructured blends of organic/polymeric photovoltaic electron donor (D) and electron acceptor (A) sandwiched by two electrodes have attracted significant attention due to the unique potential to fabricate large area flexible solar cells *via* low-cost solution processing.[3–5] With the persistent efforts in the development of the D and A materials, optimization of the device fabrication process and device configurations *etc.* in the past few decades,[6–15] OSCs, especially those from non-fullerene acceptors paired with wide band gap conjugated polymer donors (NFAs-OSCs), have provided the highest certified efficiency of 20.2% with 22–25% in sight.[16–20] However, the efficiencies of the NFAs-OSCs are still considerably lower than those of 26.3–27.5% for their counterpart inorganic or inorganic–organic hybrid solar cells because of the significantly larger non-radiative energy losses in NFAs-OSCs compared to their inorganic and hybrid counterparts,[16–22] and the minimization of the non-radiative energy losses in

[a] *Organic Semiconductor Materials and Applied Technology Research Centre of Gansu Province, School of Materials Science and Engineering, Lanzhou Jiaotong University, Lanzhou 730070, P. R. China*
[b] *Key Laboratory of Optoelectronic Chemical Materials and Devices (Ministry of Education), School of Optoelectronic Materials and Technology, Jianghan University, Wuhan 430056, P. R. China*
[c] *Department of Chemistry, KU-KIST Graduate School of Converging Science and Technology, Korea University, Seoul 02841, Republic of Korea*
[d] *Department of Chemistry and Chemical Engineering, Chalmers University of Technology, SE-41296 Göteborg, Sweden*
† These authors contributed equally.

NFAs-OSCs represents the primary challenge to achieving superior performance benchmarks.[23–28]

To address the challenge of non-radiative energy loss ($\Delta V_{oc}^{non\text{-}rad}$) in NFAs-OSCs, a range of advanced strategies have been proposed, such as morphology optimization of the photoactive layer, molecular engineering of the D and A materials, and forging the NFAs-OSCs from multi-component photovoltaic material systems.[16,18,29–40] For example, Janssen, Ma, Yang, Zhang and Chen *et al.* employed solvent or solid additives to optimize the morphology and charge transfer *etc.*, and thus the $\Delta V_{oc}^{non\text{-}rad}$ of the OSCs was decreased, and the performance of the devices was improved.[29–33] Alternatively, Li, Ma and Chen *et al.* separately achieved fast charge separation and low non-radiative recombination loss in NFAs-OSCs by rational fluorination molecular engineering of the D and/or A materials.[34–37] Kim *et al.* developed a block terpolymer *via* stepwise polymerization that combined rigid D18 and flexible PEHDT moieties, thereby reducing $\Delta V_{oc}^{non\text{-}rad}$ and enhancing the PCE from 17.78% to 19.03% to surpass the control devices from unmodified D18.[38] Tang *et al.* proposed that increasing the donor/acceptor (D/A) distance in the active layer could suppress $\Delta V_{oc}^{non\text{-}rad}$ in NFAs-OSCs.[39] Besides, Hou, Li, and Liu *et al.* reported that the $\Delta V_{oc}^{non\text{-}rad}$ of NFAs-OACs could be effectively suppressed by employing a third component or introducing additives, achieving power conversion efficiencies of up to 19.0–20.2%.[16,18,40]

Beyond the above-outlined strategies, an alternating nitroxide radical conjugated copolymer (R-CP) with the name GDTA, which was derived from 4,8-bis(4,5-dioctylthiophen-2-yl)-benzo[1,2-*b*:4,5-′]dithiophene (DBT) and *p*-phthalic acid bis(4-oxy-2,2,6,6-tetramethylpiperidine-1-oxyl)ester (BTMP), was developed and used as an additive to improve the $\Delta V_{oc}^{non\text{-}rad}$ of NFAs-OSCs by our group very recently. It was found that, upon the utilization of GDTA additives, the population of the low-lying radiative energy loss of the NFAs-OSCs from the representative organic photovoltaic D:A pair of PM6:Y6 was minimized, therefore leading to the improvement of the PCEs of the NFAs-OSCs, alongside an increase in the photo/thermal stability. Moreover, the general efficacy of GDTA additives in improving the $\Delta V_{oc}^{non\text{-}rad}$ of NFAs-OSCs is verified across NFAs-OSCs from blends of a broad range of polymer donors and non-fullerene photovoltaic pairs.[41] Encouraged by the promising effects of R-CP additives for enhancing the efficiency and stability of NFAs-OSCs, we further optimized GDTA by deliberately adjusting the content of nitroxide radical moieties in the GDTA. As a result, highly efficient NFAs-OSCs based on D18-Cl:L8-BO blends with a PCE of 19.32%, alongside simultaneous improvements in both device efficiency and operational stability by employing the optimized R-CP as additives, were achieved.[42] Moreover, the GDTA additives are also expanded to NFAs-OSCs from a wide variety of D:A blends, and simultaneous enhancements in both device efficiency and stability are further verified.[43–45]

In this study, racemic (*Rac*) and isotactic (*R* and *S*) polymonothiocarbonates with 4-oxy-2,2,6,6-tetramethyl piperidine-1-oxyl side chains, denoted as PTC-NOs, namely *Rac*-PTC-NO, (*R*)-PTC-NO, and (*S*)-PTC-NO, are employed as solid additives to mitigate non-radiative energy loss in NFAs-OSCs.

With the addition of only 0.5 wt% of *Rac*-PTC-NO, (*R*)-PTC-NO, or (*S*)-PTC-NO relative to the weight of PM6 in the active layer of PM6:Y6-based NFAs-OSCs, the PCEs were respectively increased from 15.73% to 16.59%, 17.30% and 17.40%, alongside improving the photo/thermal stability of the cells. Moreover, the enhancement of the exciton dissociation, suppression of the bimolecular recombination and trap-assisted recombination of the charge carriers, and improvement of the $\Delta V_{oc}^{non\text{-}rad}$ in the NFAs-OSCs upon the addition of the PTC-NOs additives, were verified by a set of physical measurements, such as light-intensity-dependent V_{OC} and J_{SC} analyses (V_{OC}–P_{light} J_{SC}–P_{light}), Fourier-transform photocurrent spectroscopy external quantum efficiency (FTPS-EQE) and electroluminescence external quantum efficiency (EQE_{EL}), *etc.*

2. Results and discussion

2.1 Synthesis and characterization of the PTC-NOs

The synthetic routes of the monomers of racemic 4-glycidyloxy-2,2,6,6-tetramethyl piperidine-1-oxyl (GTEMPO), (*R*)-4-glycidyloxy-2,2,6,6-tetramethylpiperidine-1-oxyl ((*R*)-GTEMPO), (*S*)-4-glycidyloxy-2,2,6,6-tetramethylpiperidine-1-oxyl ((*S*)-GTEMPO),[46] and the racemic and isotactic polymonothiocarbonates with 2,2,6,6-tetramethylpiperidine-1-oxyl side chains (PTC-NOs) with the names *Rac*-PTC-NO, (*R*)-PTC-NO and (*S*)-PTC-NO), are depicted in Scheme S1. The monomers of GTEMPO, (*R*)-GTEMPO and (*S*)-GTEMPO are prepared with the yield of 70–71% following the optimized procedure in the literature, in which tetrabutylammonium bromide was used as a phase transfer catalyst instead of tetrabutylammonium hydrogen sulfate, and characterized by measurement of the ^{1}H NMR spectra of the reduction products by erythorbic acid under ambient temperature before use (Fig. S1–S3). The PTC-NOs, *Rac*-PTC-NO, (*R*)-PTC-NO and (*S*)-PTC-NO, are respectively synthesized from GTEMPO, (*R*)-GTEMPO and (*S*)-GTEMPO with carbonyl sulfide through a (salen)CrCl/PPNCl-catalyzed polymerization reaction with the yield of 74%, 76% and 77% under 1.0 MPa.[47] The number average molecular weight (M_n) and polydispersity index (PDI) of the polymers were determined to be 5425 g mol^{-1} and 1.7 for *Rac*-PTC-NO, 3031 g mol^{-1} and 1.5 for (*R*)-PTC-NO, and 3562 g mol^{-1} and 1.6 for (*S*)-PTC-NO, by gel permeation chromatography (GPC) with THF as the eluent solvent and polystyrene standards (Fig. S4–S6). Fig. 1a shows the electron paramagnetic resonance (EPR) spectra of the polymers in chloroform solution and the solid state. In the dilute chloroform solution, all three polymers present almost the same hyperfine structures with a $g(Q)$ value of 2.006, where 3 EPR peaks interpreted in terms of the hyperfine coupling of the unpaired electron in N–O with ^{14}N nucleus spin in the TEMPO radicals are monitored (Fig. 1a).[48,49]

Meanwhile, the optical rotations and the cyclic voltammetry curves of the *Rac*-PTC-NO, (*R*)-PTC-NO and (*S*)-PTC-NO were also measured. As shown in Table S1, the optical rotations are determined to be 0° for *Rac*-PTC-NO, +21° for (*R*)-PTC-NO, and −21° for (*S*)-PTC-NO in dichloromethane solution with the concentration of 10 mg mL^{-1} *via* a Rudolph AUTOPOL

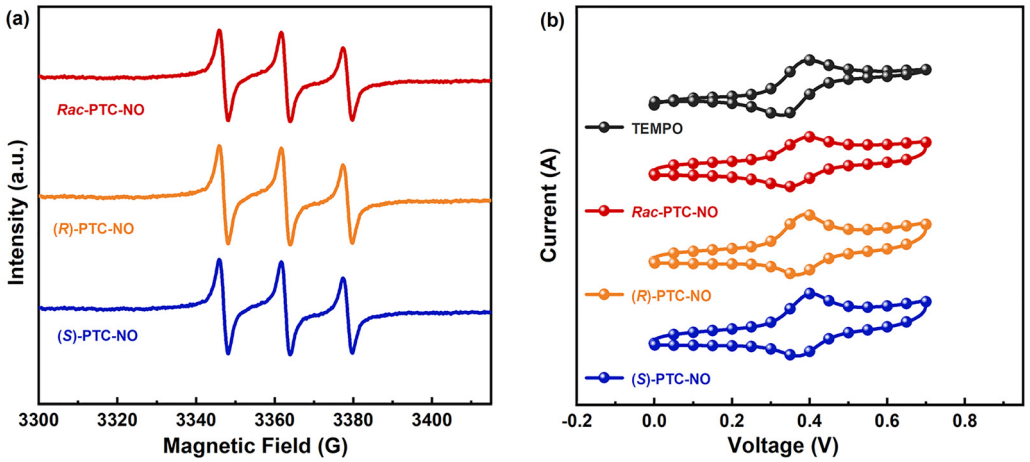

Fig. 1 EPR spectra of *Rac*-PTC-NO, (*R*)-PTC-NO and (*S*)-PTC-NO additives in (a) chloroform solution, and (b) cyclic voltammograms.

polarimeter under ambient temperature. Furthermore, the characteristic oxidation potential observed at approximately +0.28 V in the PTC-NOs (Fig. 1b) is attributed to the oxidation of the dangling TEMPO moieties, which are monitored. The thermal stability of the PTC-NOs was evaluated using thermogravimetric analysis (TGA). The results demonstrated that these polymers exhibit good thermal stability, with the temperature corresponding to 80% weight retention (T_{d80}), determined to be approximately 220 °C (Fig. S7).[47] These results unambiguously confirmed the successful synthesis of *Rac*-PTC-NO, (*R*)-PTC-NO, and (*S*)-PTC-NO.

2.2 Photovoltaic properties of the NFAs-OSCs with PTC-NOs additives

To evaluate the potential application of the PTC-NOs as solid additives to improve the performance of the NFAs-OSCs, devices with the configuration of ITO/PEDOT:PSS/PM6:Y6/PDINN/Ag (Fig. 2a), in which the PM6, Y6 and PTC-NOs polymers are, respectively, employed as the electron donor, acceptor and solid additives (Fig. 2b), and the thickness of the blend films was fixed at about 110 nm and the weight ratio of the PM6 and Y6 was about 1 : 1.2, were fabricated following the procedures in the literature.[7,41–45] The typical current density–voltage (*J*–*V*) curves and the resulting photovoltaic parameters of the optimal devices are displayed and summarized in Fig. 2c and Table 1, respectively. As shown in Fig. 2c and Table 1, the NFAs-OSCs from the pristine blends of PM6 and Y6 presented PCEs of 15.73%, along with the open circuit voltage (V_{OC}) of 0.840 V, short current density (J_{SC}) of 25.45 mA cm^{-2} and fill factor (FF) of 73.68%, while 0.5% 1-chloronaphthalene (CN) (v/v) was employed as a solid additive followed by the annealing of the blend films at 110 °C for 10 min. Under the same conditions, the PCEs of the NFAs-OSCs from the blends of PM6:Y6 with *Rac*-PTC-NO additives are improved from 15.73% to 16.59%, then dropped to 14.97%, alongside the variation of the V_{OC}s from 0.840 V to 0.853 V and 0.844 V, J_{SC}s from 25.45 mA cm^{-2} to 25.15 mA cm^{-2} and 24.21 mA cm^{-2}, and FFs from 73.59% to 77.34% and 75.91% upon the variation of the addition amount of the *Rac*-PTC-NO relative to PM6 from 0 to 0.5 wt%, and then up to 5.0 wt% (Table S2). Similar to the case of *Rac*-PTC-NO, the addition of (*R*)-PTC-NO and (*S*)-PTC-NO also led to an initial enhancement in the PCEs of the NFAs-OSCs from PM6:Y6, followed by a reduction as the additive content increases from 0 to 5% (Tables S3 and S4). Notably, devices containing 0.5 wt% of (*R*)-PTC-NO and (*S*)-PTC-NO achieved maximum PCEs of 17.30% and 17.40%, respectively, along with open-circuit V_{OC} of 0.852 V and 0.855 V, J_{SC} of 26.82–26.85 mA cm^{-2} and FF of 75.63%–75.89%, which are considerably higher than those of 15.73% for the NFAs-OSCs from pristine PM6:Y6 blends, and the devices with 0.5 wt% of *Rac*-PTC-NO additives. This suggested that PTC-NOs, especially the isotactic PTC-NOs of (*R*)-PTC-NO and (*S*)-PTC-NO can use efficient solid additives to improve the PCEs of the NFAs-OSCs similar to the utilization of the nitroxide radical conjugated polymer of the GDTA additives.[41,42]

Fig. 2d shows the external quantum efficiencies (EQEs) of the optimal NFAs-OSCs with and without 0.5 wt% PTC-NOs additives. As shown in Fig. 2d, the NFAs-OSCs from pristine PM6:Y6 blends exhibit extensive light response from 330 nm to 900 nm with the EQEs ranging from 5% to 81.1%. For comparison, the NFAs-OSCs from PM6:Y6 with *Rac*-PTC-NO, (*R*)-PTC-NO and (*S*)-PTC-NO additives present similar EQEs curves to that for the devices without additives, except that the EQEs ranging from 450 nm to 810 nm are considerably increased, alongside a slight improvement in the 350 nm–390 nm range. Likewise, the integrated current densities from all the devices show a deviation of only 5.0% as compared to those from *J*–*V* measurements. These close agreements validate the accuracy of our *J*–*V* data.[50,51]

2.3 Stability of the NFAs-OSCs with PTC-NOs additives

The photostability of the NFAs-OSCs from PM6:Y6 blends was systematically investigated to confirm the stabilizing effects of the PTC-NOs additives. This comparative study examined devices fabricated from pristine PM6:Y6 blends alongside those incorporating 0.5 wt% of *Rac*-PTC-NO, (*R*)-PTC-NO, and

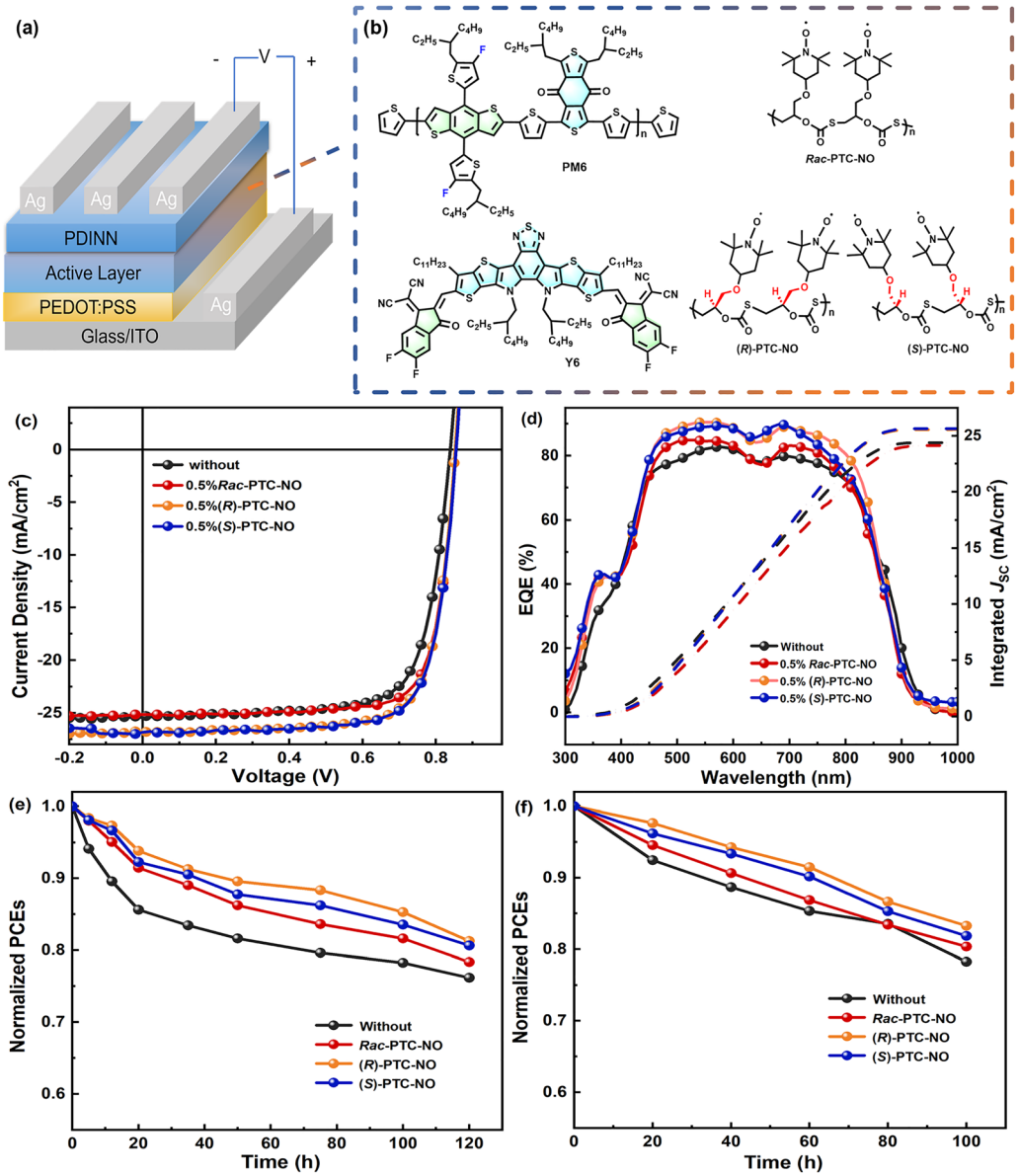

Fig. 2 (a) Device structure. (b) Chemical structures of PM6, Y6, *Rac*-PTC-NO, (*R*)-PTC-NO, and (*S*)-PTC-NO. (c) *J*/*V*, (d) EQEs, (e) photo-stability and (f) thermal stability of the NFA-OSC devices from PM6:Y6 films with and without 0.5 wt% of *Rac*-PTC-NO, (*R*)-PTC-NO and (*S*)-PTC-NO additives.

Table 1 Photovoltaic parameters of the NFAs-OSCs from PM6:Y6 blends with and without 0.5 wt% *Rac*-PTC-NO, (*R*)-PTC-NO, and (*S*)-PTC-NO

Active layer	Additive	J_{SC} (mA cm^{-2})	V_{OC} (V)	FF (%)	PCE (%)	Cal. J_{SC} (mA cm^{-2})
PM6:Y6	Without	25.45	0.839	73.68	15.73	24.38
	0.5 wt% of *Rac*-PTC-NO	25.15	0.853	77.34	16.59	24.14
	0.5 wt% of (*R*)-PTC-NO	26.85	0.852	75.63	17.30	25.56
	0.5 wt% of (*S*)-PTC-NO	26.82	0.855	75.89	17.40	25.65

(*S*)-PTC-NO additives. All devices underwent accelerated aging under simulated 1-sun illumination (100 mW cm^{-2}) provided by a white LED light source with a color temperature of 6000 K and spectral range of 400–800 nm. Meanwhile, the testing was conducted in a carefully controlled glovebox environment with oxygen and water concentrations maintained below 1 ppm to eliminate atmospheric degradation effects. According to the results presented in Fig. 2e, the control devices from the pristine PM6:Y6 blends showed substantial performance degradation, with their PCEs decreasing by 23.84% after 120 hours of continuous irradiation. In contrast, the devices with 0.5 wt% of *Rac*-PTC-NO, (*R*)-PTC-NO, and (*S*)-PTC-NO additives maintained

considerably higher stability, with PCE losses of only 21.66%, 18.73%, and 19.37% after 120 hours of continuous irradiation, respectively.

In parallel, the thermal stability of the NFAs-OSCs was similarly evaluated by comparing the PCEs of the cells from the pristine PM6:Y6 blends with those with 0.5 wt% of *Rac*-PTC-NO, (*R*)-PTC-NO, and (*S*)-PTC-NO additives. As depicted in Fig. 2f, the NFAs-OSCs from the pristine PM6:Y6 blends exhibited a 21.75% reduction in PCE after 100 hours of thermal aging at 60 °C in a nitrogen-filled glovebox. Under the same conditions, the addition of 0.5 wt% of *Rac*-PTC-NO, (*R*)-PTC-NO, and (*S*)-PTC-NO additives demonstrated a stabilizing effect, with PCEs losses of 19.64%, 16.73% and 18.13%, for the 0.5 wt% *Rac*-PTC-NO, (*S*)-PTC-NO, and (*R*)-PTC-NO modified NFAs-OSCs from PM6:Y6 blends, respectively. With these results, it could be found that, similar to the utilization of the GDTA additives, the addition of the *Rac*-PTC-NO, (*R*)-PTC-NO, and (*S*)-PTC-NO additives effectively enhances both photostability and thermal stability in NFAs-OSCs.[41]

2.4 Influence of the light harvesting, morphology and charge transporting behaviors of the NFAs-OSCs from PM6:Y6 with PTC-NOs additives

To elucidate the performance enhancement of NFAs-OSCs with 0.5 wt% PTC-NOs additives, a series of systematic investigations were conducted on PM6:Y6 blend films with and without these additives. Firstly, the UV-vis absorption measurements confirm that the addition of the 0.5 wt% PTC-NOs additives cause no significant changes in absorptance spectra, indicating preserved light-harvesting capabilities (Fig. S8). Additionally, as shown in Fig. 3a and b, the pristine PM6:Y6 blend without PTC-NOs additives exhibited a strong in-plane (IP) diffraction peak at q = 0.286 Å^{-1} (d-spacing = 21.969 Å), corresponding to the lamellar stacking of either PM6 or Y6. In the out-of-plane (OOP) direction, a strong diffraction peak at q = 1.704 Å^{-1} (d-spacing = 3.687 Å^{-1}), which is assigned to the π–π stacking of Y6, is observed.[7,41,42] In contrast, the PM6:Y6 blends with PTC-NOs additives show peak shifts in both directions. Specifically, the *Rac*-PTC-NO modified blend displays IP and OOP peaks at q = 0.288 Å^{-1} and 1.709 Å^{-1}. And the (*R*)-PTC-NO and (*S*)-PTC-NO modified blends exhibit further shifts to q = 0.294 Å^{-1}/1.716 Å^{-1} and q = 0.292 Å^{-1}/1.714 Å^{-1}, respectively. The OOP and IP crystalline coherence length (CCL) values of 31.593–31.954 Å and 96.247–97.084 Å for the PM6:Y6 films with 0.5 wt% of *Rac*-PTC-NO, (*R*)-PTC-NO and (*S*)-PTC-NO additives are higher than those of 30.065 Å and 91.974 Å for the pristine PM6:Y6 films (Table S5). At the same time, atomic force microscopy (AFM) and transmission electron microscopy (TEM) measurements confirm comparable surface characteristics in the PM6:Y6 films, showing slightly lower root mean square (RMS) roughness values, ranging from 1.014 nm to 1.186 nm in contrast to that of 1.247 nm upon the addition of the PTC-NOs additives, along with slightly refined morphological textures as compared to that for the pristine PM6:Y6 films without additives (Fig. 3c and d).

Afterwards, the charge transporting characteristics of the PM6:Y6 blend films with and without 0.5 wt% of PTC-NOs additives were also measured using the space-charge-limited-current (SCLC) method.[52,53] As shown in Fig. 3e and f and Table S6, the pristine PM6:Y6 films exhibited a hole mobility of 4.03 × 10^{-4} cm^2 V^{-1} s^{-1} and an electron mobility of 2.22 × 10^{-4} cm^2 V^{-1} s^{-1}, with a corresponding μ_h/μ_e ratio of 1.82. For comparison, the *Rac*-PTC-NO, (*R*)-PTC-NO, and (*S*)-PTC-NO additive optimized devices demonstrated three distinct performance regimes: hole/electron mobilities of 5.45 × 10^{-4}/3.08 × 10^{-4} cm^2 V^{-1} s^{-1} (μ_h/μ_e = 1.78), 5.52 × 10^{-4}/4.17 × 10^{-4} cm^2 V^{-1} s^{-1} (μ_h/μ_e = 1.32), and 5.75 × 10^{-4}/3.98 × 10^{-4} cm^2 V^{-1} s^{-1} (μ_h/μ_e = 1.44), respectively. Based on the above results, it can be tentatively concluded that, while the addition of PTC-NOs additives leaves the light-harvesting properties and surface roughness of PM6:Y6-based films largely unaffected, it induces modest enhancements in charge mobility, balanced hole and electron transport, crystalline coherence length, and morphological texture as well. These factors might result in improved charge carrier transport and decreased charge carriers' recombination in the devices, contributing to the observed performance gains of the NFAs-OSCs.[40,41] However, it would be premature to conclusively ascribe the elevated device metrics of PCE, V_{OC}, J_{SC}, and FF exclusively to these minor morphological alterations upon the addition of PTC-NOs additives.

2.5 Exciton dissociation probability and charge carrier recombination of PM6:Y6-based NFAs-OSCs with and without PTC-NOs additive

Fig. 4a and b present the photocurrent density *versus* effective voltage (J_{ph}–V_{eff}) curves and the corresponding exciton dissociation probability ($P(E,T)$) for PM6:Y6-based NFAs-OSCs with and without 0.5 wt% of PTC-NOs additives. The exciton dissociation probability is determined by the equation of $P(E,T) = J_{ph}/J_{sat}$, in which J_{sat} represents the saturation current density, $J_{ph} = J_L - J_d$, and $V_{eff} = V_0 - V$ (V_0 being the voltage at J_{ph} = 0).[54–56] As shown in Fig. 4a, the saturations in the photocurrent density are observed at high effective voltages ($V_{eff} > 3$ V), beyond which no further increase in J_{ph} occurred. When the $V_{eff} \approx 4$ V, J_{ph} reaches saturation implying that photogenerated excitons undergo complete dissociation into free charge carriers, which are efficiently collected at the electrodes. As shown in Fig. 4b, the NFAs-OSCs from pristine PM6:Y6 films without additives provide a $P(E,T)$ value of 92.73%, which is increased to 93.11% for *Rac*-PTC-NO, 94.28% for (*R*)-PTC-NO, and 93.46% for (*S*)-PTC-NO. This systematic improvement in exciton dissociation efficiency might directly contribute to the enhanced J_{SC}s and PCEs of the devices with the PTC-NOs additives.

Fig. 4c and d present the relationship of the J_{SC}s and V_{OC}s of the NFAs-OSCs of PM6:Y6 with and without 0.5 wt% PTC-NOs additives under varying light intensities (P_{light}). The bimolecular recombination of the charge carriers in the NFAs-OSCs is assessed by the degree of J_{SC}s and P_{light} ($J_{SC} \propto P_{light}$)$^{\alpha}$, where α

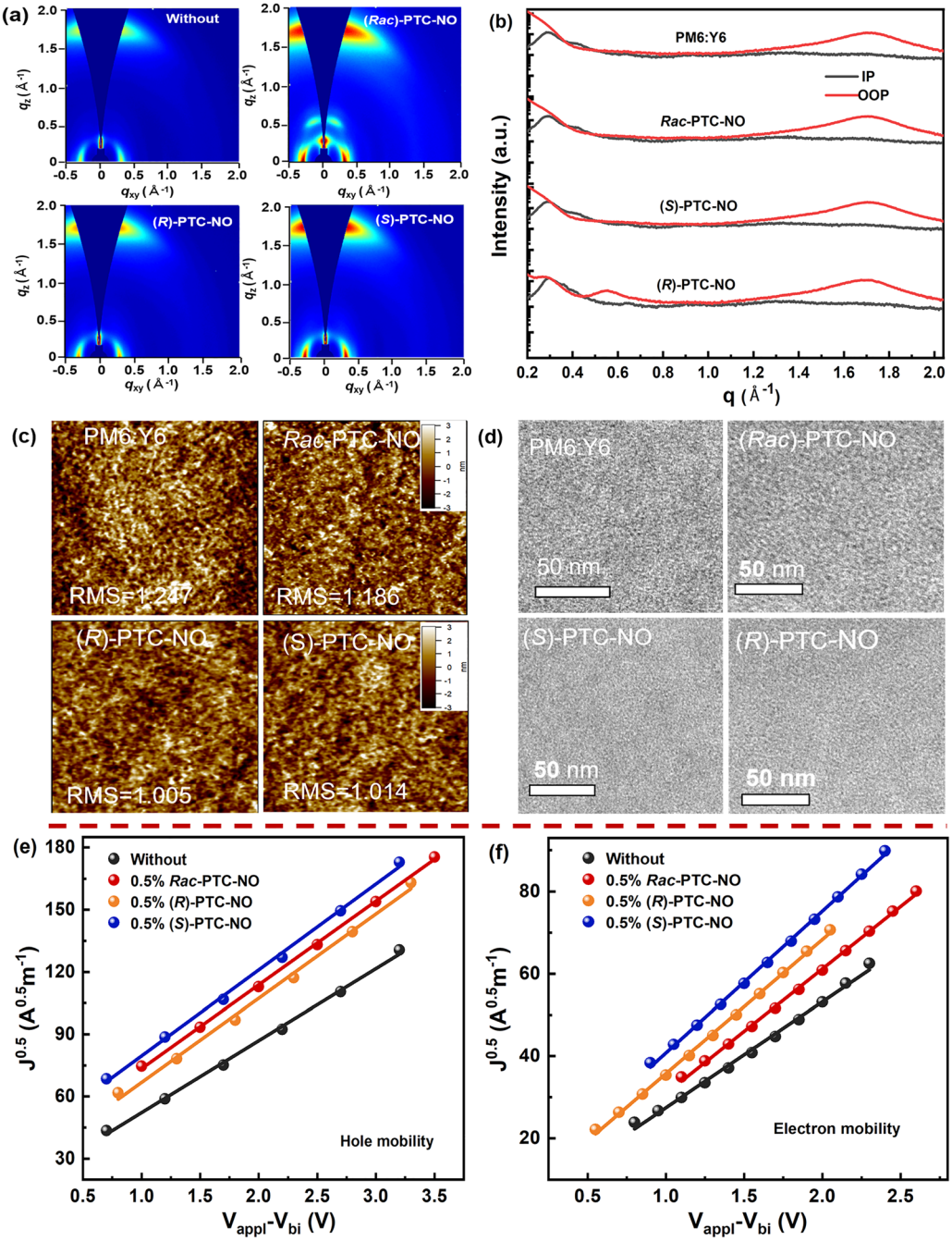

Fig. 3 Morphology characteristics of the PM6:Y6 films without and with 0.5 wt% of *Rac*-PTC-NO, (*R*)-PTC-NO and (*S*)-PTC-NO additives. (a) 2D-GIWAXS images, (b) corresponding line-cuts along the in-plane (IP, top) and out-of-plane (OOP, bottom) direction, (c) AFM (5 μm × 5 μm), (d) TEM images, (e) hole mobility, and (f) electron mobility.

values closer to 1 indicate suppressed recombination.[31,57] Likewise, the slope of the trap-assisted recombination was between KT/q and $2KT/q$, as evaluated from the slope n in the relationship $V_{OC} \propto (nkT/q)\ln(P_{light})$, with k, T, and q denoting the Boltzmann constant, absolute temperature, and elementary charge, respectively. And the n values approaching 1 for the devices usually signifies reduced trap-assisted recombination.[41,44] As shown in Fig. 4c and d, the α and n values of the devices with 0.5 wt% *Rac*-PTC-NO, (*R*)-PTC-NO, and (*S*)-PTC-NO additives were, respectively, determined to be 0.954 and 1.19, 0.974 and 1.07, and 0.967 and 1.15. Compared to the control PM6:Y6 NFAs-OSCs (α = 0.927, n = 1.27), the NFAs-OSCs with 0.5 wt% of PTC-NOs additive exhibit α and n values closer to 1. These results indicate that the addition of PTC-NOs additives can effectively suppress both bimolecular and trap-assisted recombination.

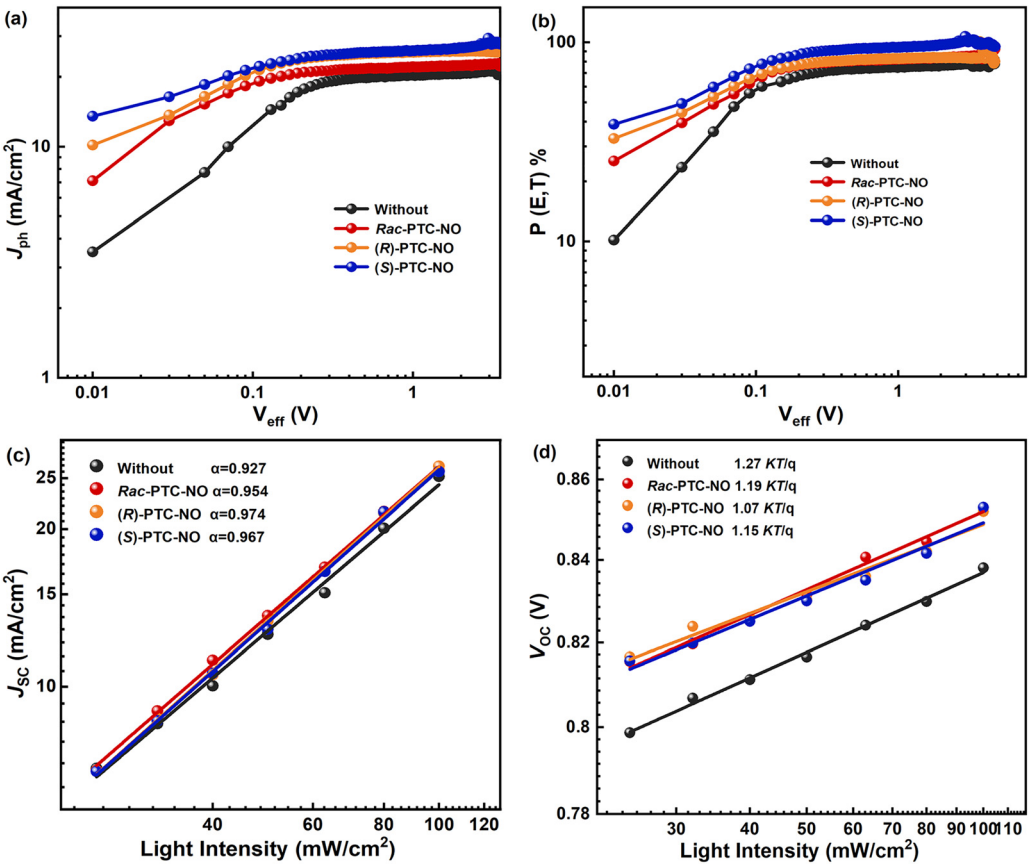

Fig. 4 (a) J_{SC}–P_{light}, (b) V_{OC}–P_{light}, (c) J_{ph}–V_{eff} and (d) $P(E,T)$–V_{eff} of NFAs-OSCs from the PM6:Y6 blends with and without 0.5 wt% of *Rac*-PTC-NO, (*R*)-PTC-NO and (*S*)-PTC-NO additives.

2.6 Reduction of non-radiative energy loss of the PM6:Y6 OSCs upon the addition of PTC-NOs

To get insight into the improvement of the V_{OC}s for the PM6:Y6-based NFAs-OSCs upon the addition of PTC-NOs additives, the Fourier-transform photocurrent spectroscopy external quantum efficiency (FTPS-EQE), electroluminescence (EL) spectra, and electroluminescence external quantum efficiency (EQE_{EL}) of the NFAs-OSCs were measured and analyzed *via* the detailed balance theory.[26,32,41,58–60] As shown in Fig. 5a–e and Table 2, all the devices exhibited nearly identical EL and FTPS-EQE spectra with similar radiative losses. However, the EQE_{EL} values for the pristine PM6:Y6 devices and the devices with 0.5 wt% *Rac*-PTC-NO, 0.5 wt% (*R*)-PTC-NO and 0.5 wt% (*S*)-PTC-NO additives were measured to be 6.61×10^{-3}%, 8.91×10^{-3}%, 9.42×10^{-3}% and 9.53×10^{-3}%, respectively. The corresponding non-radiative voltage loss ($\Delta V_{oc}^{non\text{-}rad}$), calculated using $V_{oc}^{non\text{-}rad} = -\frac{kT}{q}\ln(EQE_{EL})$,[26] was 0.255 for the pristine PM6:Y6 devices, compared to 0.242, 0.241 and 0.240 for the modified devices. These results demonstrate that the incorporation of PTC-NOs additives efficiently decreased the $\Delta V_{oc}^{non\text{-}rad}$ of the PM6:Y6-based NFAs-OSCs, thus resulting in the improvement of the V_{OC}s. Based on all the opto-electronic investigations of PM6:Y6 blend films and NFAs-OSCs from them, it can be speculated that PTC-NOs additives, like the nitroxide radical polymer GDTA additive,[41] presumably suppress the singlet-to-triplet charge transfer (^{1}CT → ^{3}CT) transition. This reduces the ^{3}CT population, thereby slowing the back charge transfer to the triplet state (T_1) on Y6 and decreasing the T_1 population. Consequently, both charge recombination *via* triplet-charge annihilation and non-radiative energy loss *via* T_1 are mitigated. These effects collectively enhance the PCE, V_{OC}s, J_{SC}s, and FF of the NFAs-OSCs.[41,58–60]

3. Conclusions

In summary, racemic and isotactic nitroxide radical polymonothiocarbonates (*Rac*-/(*R*)-/(*S*)-PTC-NO) have been demonstrated as effective solid additives for NFAs-OSCs. The incorporation of merely 0.5 wt% of these additives resulted in a substantial enhancement in device performance, with the power conversion efficiencies (PCEs) increasing from a baseline of 15.73% for NFAs-OSCs without additives to 16.59%, 17.30% and 17.40% for devices containing *Rac*-PTC-NO, (*R*)-PTC-NO,

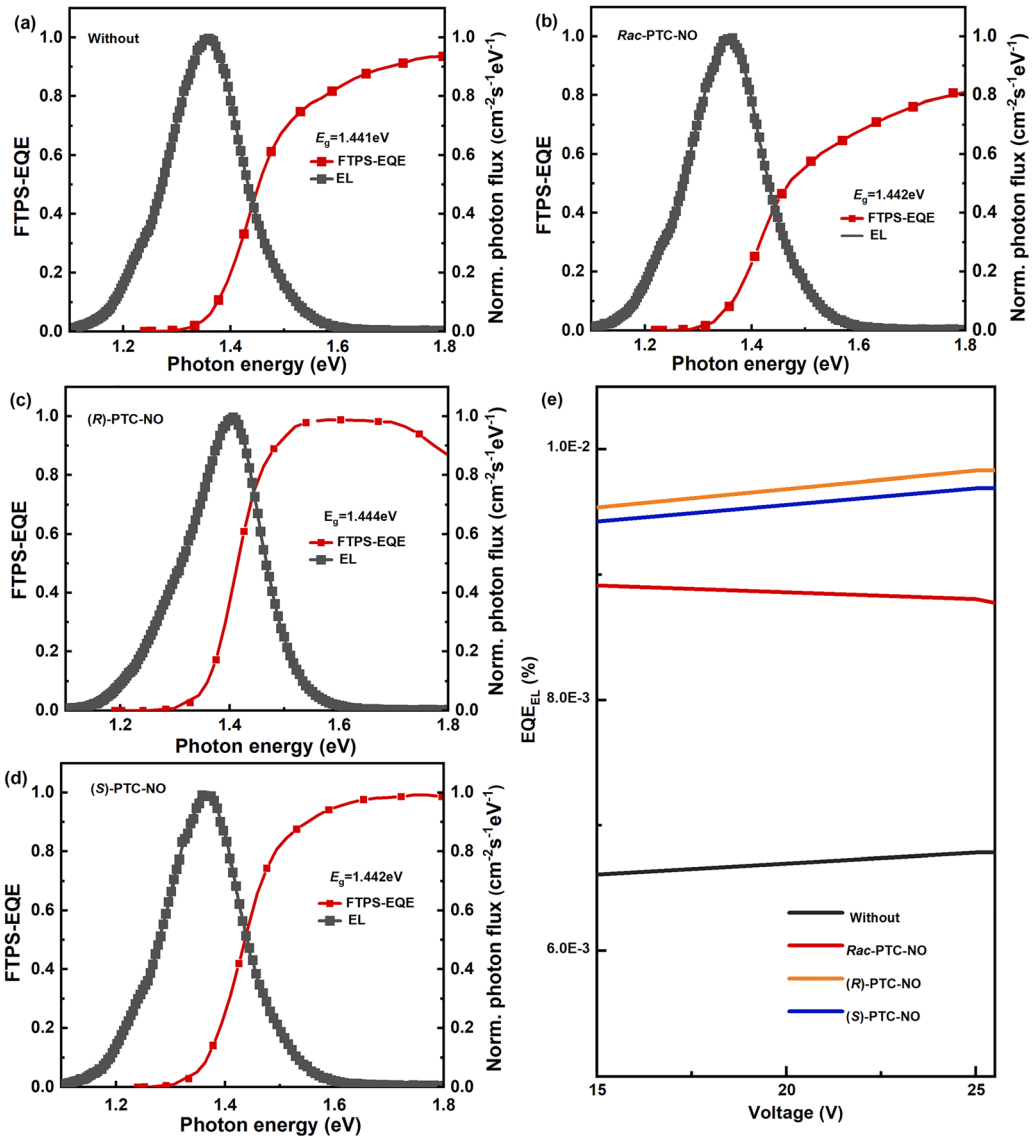

Fig. 5 EL, FTPS-EQE spectra (a)–(d) and EQE_{EL} (e) of NFAs-OSCs from the PM6:Y6 blends with and without 0.5 wt% of *Rac*-PTC-NO, (*R*)-PTC-NO and (*S*)-PTC-NO additives.

Table 2 Total and detailed voltage loss of NFAs-OSCs based on PM6:Y6 blends with and without 0.5 wt% of *Rac*-PTC-NO, (*R*)-PTC-NO and (*S*)-PTC-NO additives

Active layer	Additive	E_g (eV)	qV_{OC}^{SQ} (eV)	ΔE_1 (eV)	qV_{OC}^{rad} (eV)	ΔE_2 (eV)	EQE_{EL} (%)	$q\Delta V_{oc}^{non\text{-}rad}$ (eV)	qV_{OC}^{Cal} (V)
PM6:Y6	Without	1.441	1.174	0.267	1.094	0.079	6.61×10^{-3}	0.255	0.840
	Rac-PTC-NO	1.442	1.175	0.267	1.096	0.080	8.91×10^{-3}	0.242	0.853
	(*R*)-PTC-NO	1.442	1.174	0.268	1.088	0.080	9.42×10^{-3}	0.241	0.853
	(*S*)-PTC-NO	1.443	1.176	0.268	1.126	0.081	9.53×10^{-3}	0.240	0.855

and (*S*)-PTC-NO, respectively. Concurrently, the devices exhibited improved thermal and photo-stability, indicating the dual function of these additives in boosting both efficiency and stability. The underlying reasons for these improvements were elucidated through a suite of physical measurements, including absorption spectra, morphology, and charge transport characteristics of the PM6:Y6 blends, as well as the light-intensity-dependent open-circuit voltage (V_{OC}–P_{light}), light-intensity-dependent short-circuit current (J_{SC}–P_{light}), Fourier-transform photocurrent spectroscopy external quantum efficiency (FTPS-EQE), and electroluminescence external quantum efficiency (EQE_{EL}) of the devices upon the addition of the PTC-NOs additives. Together, these results point to a significant performance enhancement in the NFAs-OSCs arising from the

PTC-NOs additives, which concurrently enhance exciton dissociation, suppress bimolecular/trap-assisted recombination, and minimize non-radiative energy loss.

Author contributions

Yuyan Tao: methodology, data curation, and writing – original draft. Xuanyu Zhou: formal analysis and data curation. Xiao Zheng and Huiyuan Peng: data curation. Min Gyu Kang and Hanyoung Woo: investigation. Pengzhi Guo: formal analysis. Xunchang Wang: investigation and methodology. Renqiang Yang: formal analysis. Yangjun Xia: writing, review and editing, validation, funding acquisition, and conceptualization. Ergang Wang: resources and formal analysis.

Conflicts of interest

The authors declare no conflicts of interest.

Data availability

All data generated or analyzed during this study are included in this published article and its supplementary information (SI). Supplementary information: materials, general experiments, preparation and characterization of the organic solar cells, and synthesis of the *Rac*-PTC-NO, (*R*)-PTC-NO, and (*S*)-PTC-NO polymers. See DOI: https://doi.org/10.1039/d6ma00058d.

Acknowledgements

This work was supported by the Industrial Guidance Project for Colleges and Universities of Gansu Province (2020C-07), the National Natural Science Foundation of China (62164007) and the 2025 short-term program for high-level foreign experts.

Notes and references

1 N. S. Sariciftci, L. Smilowitz, A. J. Heeger and F. Wudl, *Science*, 1992, **258**, 1474–1476.
2 G. Yu, J. Gao, J. C. Hummelen, F. Wudl and A. J. Heeger, *Science*, 1995, **270**, 1789–1791.
3 M. M. Wienk, J. M. Kroon, W. J. H. Verhees, J. Knol, J. C. Hummelen, P. A. van Hal and R. A. J. Janssen, *Angew. Chem., Int. Ed.*, 2003, **42**, 3371–3375.
4 G. Li, V. Shrotriya, J. Huang, Y. Yao, T. Moriarty, K. Emery and Y. Yang, *Nat. Mater.*, 2005, **4**, 864–868.
5 L. Huo, T. Liu, X. Sun, Y. Cai, A. J. Heeger and Y. Sun, *Adv. Mater.*, 2015, **27**, 2938–2944.
6 Y. Lin, J. Wang, Z. Zhang, H. Bai, Y. Li, D. Zhu and X. Zhan, *Adv. Mater.*, 2015, **27**, 1170–1174.
7 J. Yuan, Y. Zhang, L. Zhou, G. Zhang, H.-L. Yip, T.-K. Lau, X. Lu, C. Zhu, H. Peng, P. A. Johnson, M. Leclerc, Y. Cao, J. Ulanski, Y. Li and Y. Zou, *Joule*, 2019, **3**, 1140–1151.
8 H. Bin, Z.-G. Zhang, L. Gao, S. Chen, L. Zhong, L. Xue, C. Yang and Y. Li, *J. Am. Chem. Soc.*, 2016, **138**, 4657–4664.
9 Z. Luo, R. Ma, T. Liu, J. Yu, Y. Xiao, R. Sun, G. Xie, J. Yuan, Y. Chen, K. Chen, G. Chai, H. Sun, J. Min, J. Zhang, Y. Zou, C. Yang, X. Lu, F. Gao and H. Yan, *Joule*, 2020, **4**, 1236–1247.
10 Z. He, C. Zhong, S. Su, M. Xu, H. Wu and Y. Cao, *Nat. Photonics*, 2012, **6**, 591–595.
11 W. Zhao, S. Li, H. Yao, S. Zhang, Y. Zhang, B. Yang and J. Hou, *J. Am. Chem. Soc.*, 2017, **139**, 7148–7151.
12 S. Li, X. Yuan, Q. Zhang, B. Li, Y. Li, J. Sun, Y. Feng, X. Zhang, Z. Wu, H. Wei, M. Wang, Y. Hu, Y. Zhang, H. Y. Woo, J. Yuan and W. Ma, *Adv. Mater.*, 2021, **33**, 2101295.
13 Q. Liu, Y. Jiang, K. Jin, J. Qin, J. Xu, W. Li, J. Xiong, J. Liu, Z. Xiao, K. Sun, S. Yang, X. Zhang and L. Ding, *Sci. Bull.*, 2020, **65**, 272–275.
14 L. Zhu, M. Zhang, J. Xu, C. Li, J. Yan, G. Zhou, W. Zhong, T. Hao, J. Song, X. Xue, Z. Zhou, R. Zeng, H. Zhu, C.-C. Chen, R. C. I. MacKenzie, Y. Zou, J. Nelson, Y. Zhang, Y. Sun and F. Liu, *Nat. Mater.*, 2022, **21**, 656–663.
15 Y. Miao, Y. Sun, W. Zou, X. Zhang, Y. Kan, W. Zhang, X. Jiang, X. Wang, R. Yang, X. Hao, L. Geng, H. Xu and K. Gao, *Adv. Mater.*, 2024, **36**, 2406623.
16 Y. Sun, L. Wang, C. Guo, J. Xiao, C. Liu, C. Chen, W. Xia, Z. Gan, J. Cheng, J. Zhou, Z. Chen, J. Zhou, D. Liu, T. Wang and W. Li, *J. Am. Chem. Soc.*, 2024, **146**, 12011–12019.
17 Y. Jiang, S. Sun, R. Xu, F. Liu, X. Miao, G. Ran, K. Liu, Y. Yi, W. Zhang and X. Zhu, *Nat. Energy*, 2024, **9**, 975–986.
18 L. Zhu, M. Zhang, G. Zhou, Z. Wang, W. Zhong, J. Zhuang, Z. Zhou, X. Gao, L. Kan, B. Hao, F. Han, R. Zeng, X. Xue, S. Xu, H. Jing, B. Xiao, H. Zhu, Y. Zhang and F. Liu, *Joule*, 2024, **8**, 3153–3168.
19 W. Zou, Y. Sun, L. Sun, X. Wang, C. Gao, D. Jiang, J. Yu, G. Zhang, H. Yin, R. Yang, H. Zhu, H. Chen and K. Gao, *Adv. Mater.*, 2025, **37**, 2413125.
20 H. Xu, X. Jiang, Y. Sun, L. Sun, W. Zou, S. Liu, S. Shen, T. Gao, C. Hong, X. Wang, C. Gao, D. Jiang, J. Zheng, X. Zou, W. Zhang, G. Zhang, H. Yin, R. Yang, D. Liu, Y. Kan and K. Gao, *Adv. Mater.*, 2026, **38**, e20639.
21 J. Park, J. Kim, H.-S. Yun, M. J. Paik, E. Noh, H. J. Mun, M. G. Kim, T. J. Shin and S. I. Seok, *Nature*, 2023, **616**, 724–730.
22 H. Chen, C. Liu, J. Xu, A. Maxwell, W. Zhou, Y. Yang, Q. Zhou, A. S. R. Bati, H. Wan, Z. Wang, L. Zeng, J. Wang, P. Serles, Y. Liu, S. Teale, Y. Liu, M. I. Saidaminov, M. Li, N. Rolston, S. Hoogland, T. Filleter, M. G. Kanatzidis, B. Chen, Z. Ning and E. H. Sargent, *Science*, 2024, **384**, 189–193.
23 M. Azzouzi, J. Yan, T. Kirchartz, K. Liu, J. Wang, H. Wu and J. Nelson, *Phys. Rev. X*, 2018, **8**, 031055.
24 A. J. Gillett, A. Privitera, R. Dilmurat, A. Karki, D. Qian, A. Pershin, G. Londi, W. K. Myers, J. Lee, J. Yuan, S.-J. Ko, M. K. Riede, F. Gao, G. C. Bazan, A. Rao, T.-Q. Nguyen, D. Beljonne and R. H. Friend, *Nature*, 2021, **597**, 666–671.
25 S. M. Hosseini, S. Wilken, B. Sun, F. Huang, S. Y. Jeong, H. Y. Woo, V. Coropceanu and S. Shoaee, *Adv. Energy Mater.*, 2023, **13**, 2203576.
26 S. Liu, J. Yuan, W. Deng, M. Luo, Y. Xie, Q. Liang, Y. Zou, Z. He, H. Wu and Y. Cao, *Nat. Photonics*, 2020, **14**, 300–305.

27 A. Armin, N. Zarrabi, O. J. Sandberg, C. Kaiser, S. Zeiske, W. Li and P. Meredith, *Adv. Energy Mater.*, 2020, **10**, 2001828.
28 Z. Chen, X. Chen, Z. Jia, G. Zhou, J. Xu, Y. Wu, X. Xia, X. Li, X. Zhang, C. Deng, Y. Zhang, X. Lu, W. Liu, C. Zhang, Y. (Michael) Yang and H. Zhu, *Joule*, 2021, **5**, 1832–1844.
29 D. Di Nuzzo, A. Aguirre, M. Shahid, V. S. Gevaerts, S. C. J. Meskers and R. A. J. Janssen, *Adv. Mater.*, 2010, **22**, 4321–4324.
30 M. Xiao, Y. Meng, L. Tang, P. Li, L. Tang, W. Zhang, B. Hu, F. Yi, T. Jia, J. Cao, C. Xu, G. Lu, X. Hao, W. Ma and Q. Fan, *Adv. Funct. Mater.*, 2024, **34**, 2311216.
31 H. Xiang, F. Sun, X. Zheng, B. Gao, P. Zhu, T. Cong, Y. Li, X. Wang and R. Yang, *Adv. Sci.*, 2024, **11**, 2401330.
32 Y. Wang, W. Sun, Y. Zhang, B. Zhang, Y. Ding, Z. Zhang, L. Meng, K. Huang, W. Ma and H. Zhang, *Angew. Chem., Int. Ed.*, 2025, **64**, e202417643.
33 Z. Li, L. Zhan, H. Qiu, X. Sun, H. Hu, R. Gui, H. Yin, R. Sun, J. Min, J. Yu, W. Fu, W. Qiu, Z.-X. Liu, S. Yin and H. Chen, *Energy Environ. Sci.*, 2024, **17**, 8293–8303.
34 C. Sun, F. Pan, S. Chen, R. Wang, R. Sun, Z. Shang, B. Qiu, J. Min, M. Lv, L. Meng, C. Zhang, M. Xiao, C. Yang and Y. Li, *Adv. Mater.*, 2019, **31**, 1905480.
35 R. Wang, J. Xu, L. Fu, C. Zhang, Q. Li, J. Yao, X. Li, C. Sun, Z.-G. Zhang, X. Wang, Y. Li, J. Ma and M. Xiao, *J. Am. Chem. Soc.*, 2021, **143**, 4359–4366.
36 L. Xue, Y. Yang, J. Xu, C. Zhang, H. Bin, Z.-G. Zhang, B. Qiu, X. Li, C. Sun, L. Gao, J. Yao, X. Chen, Y. Yang, M. Xiao and Y. Li, *Adv. Mater.*, 2017, **29**, 1703344.
37 X. Si, Y. Huang, W. Shi, R. Wang, K. Ma, Y. Zhang, S. Wu, Z. Yao, C. Li, X. Wan and Y. Chen, *Adv. Funct. Mater.*, 2023, **33**, 2306471.
38 J.-W. Lee, H.-G. Lee, E. S. Oh, S.-W. Lee, T. N.-L. Phan, S. Li, T.-S. Kim and B. J. Kim, *Joule*, 2024, **8**, 204–223.
39 J. Wang, X. Jiang, H. Wu, G. Feng, H. Wu, J. Li, Y. Yi, X. Feng, Z. Ma, W. Li, K. Vandewal and Z. Tang, *Nat. Commun.*, 2021, **12**, 6679.
40 P. Bi, S. Zhang, Z. Chen, Y. Xu, Y. Cui, T. Zhang, J. Ren, J. Qin, L. Hong, X. Hao and J. Hou, *Joule*, 2021, **5**, 2408–2419.
41 F. Shi, P. Guo, X. Qiao, G. Yao, T. Zhang, Q. Lu, Q. Wang, X. Wang, J. Rikhsibaev, E. Wang, C. Zhang, Y.-W. Kwon, H. Y. Woo, H. Wu, J. Hou, D. Ma, A. Armin, Y. Ma and Y. Xia, *Adv. Mater.*, 2023, **35**, 2212084.
42 P. Guo, Y. Tao, J. Liang, F. Shi, X. Wang, Z. Zhu, Y. Xiang, R. Yang, E. Wang and Y. Xia, *Chem. Eng. J.*, 2025, **512**, 162339.
43 Q. Wang, J. Guan, H. Du, X. Yang, F. Shi, D. Li, P. Guo and Y. Xia, *Polymer*, 2024, **314**, 127780.
44 H. Xu, P. Guo, Q. Wang, X. He, A. Zhou, X. Sun, E. Wang, H. Y. Woo, H. Wu and Y. Xia, *J. Mater. Chem. C*, 2024, **12**, 3644–3653.
45 H. Peng, J. Liang, Y. Zhou, Z. Zhu, J. Guan, P. Guo, X. Wang, R. Yang, E. Wang and Y. Xia, *J. Mater. Chem. C*, 2025, **13**, 6416–6424.
46 Y. Joo, V. Agarkar, S. H. Sung, B. M. Savoie and B. W. Boudouris, *Science*, 2018, **359**, 1391–1395.
47 G. A. Bhat, A. Z. Rashad, X. Ji, M. Quiroz, L. Fang and D. J. Darensbourg, *Angew. Chem.*, 2021, **133**, 20902–20906.
48 X. Pang and W. J. Jin, *New J. Chem.*, 2015, **39**, 5477–5483.
49 B. Endeward, M. Bretschneider, P. Trenkler and T. F. Prisner, *Prog. Nucl. Magn. Reson. Spectrosc.*, 2023, **136–137**, 61–82.
50 F. Liu, L. Zhou, W. Liu, Z. Zhou, Q. Yue, W. Zheng, R. Sun, W. Liu, S. Xu, H. Fan, L. Feng, Y. Yi, W. Zhang and X. Zhu, *Adv. Mater.*, 2021, **33**, 2100830.
51 C. Li, J. Zhou, J. Song, J. Xu, H. Zhang, X. Zhang, J. Guo, L. Zhu, D. Wei, G. Han, J. Min, Y. Zhang, Z. Xie, Y. Yi, H. Yan, F. Gao, F. Liu and Y. Sun, *Nat. Energy*, 2021, **6**, 605–613.
52 Y. Xu, Y. Li, S. Li, F. Balestra, G. Ghibaudo, W. Li, Y.-F. Lin, H. Sun, J. Wan, X. Wang, Y. Guo, Y. Shi and Y.-Y. Noh, *Adv. Funct. Mater.*, 2020, **30**, 2070125.
53 T. Yang, C. Liao, Y. Duan, X. Xu, M. Deng, L. Yu, R. Li and Q. Peng, *Adv. Funct. Mater.*, 2022, **32**, 2208950.
54 X. Zheng, X. Wang, F. Sun, M. Wan, Z. Li, C. Xiao, T. Cong, T. Hu, Y. Liao and R. Yang, *Chem. Eng. J.*, 2023, **475**, 145520.
55 H. Tian, W. Xu, Z. Liu, Y. Xie, W. Zhang, Y. Xu, S. Y. Jeong, F. Zhang, N. Weng, Z. Zhang, K. Wang, Q. Sun, J. Zhang, X. Li, X. Du, X. Hao, H. Y. Woo, X. Ma and F. Zhang, *Adv. Funct. Mater.*, 2024, **34**, 2313751.
56 X. Cui, G. Ran, H. Lu, Y. Liu, H. Jiang, H. Zhang, D. Li, Y. Liu, Y. Lin, Z. Ma, W. Zhang, P. Cheng and Z. Bo, *Adv. Funct. Mater.*, 2024, **34**, 2400219.
57 J. Guan, Y. Tao, A. Zhou, P. Guo, Y. Zhou, C. Zhuang, C. Wang and Y. Xia, *Macromol. Chem. Phys.*, 2025, **226**, 2400524.
58 L. J. A. Koster, M. Kemerink, M. M. Wienk, K. Maturová and R. A. J. Janssen, *Adv. Mater.*, 2011, **23**, 1670–1674.
59 S. M. Menke, N. A. Ran, G. C. Bazan and R. H. Friend, *Joule*, 2018, **2**, 25–35.
60 K. Jiang, J. Zhang, C. Zhong, F. R. Lin, F. Qi, Q. Li, Z. Peng, W. Kaminsky, S.-H. Jang, J. Yu, X. Deng, H. Hu, D. Shen, F. Gao, H. Ade, M. Xiao, C. Zhang and A. K.-Y. Jen, *Nat. Energy*, 2022, **7**, 1076–1086.